MicroRNA-34a activation in tuberous sclerosis complex during early brain development may lead to impaired corticogenesis

Korotkov, A.; Sim, N.S.; Luinenburg, M.J.; Anink, J.J.; van Scheppingen, J.; Zimmer, T.S.; Bongaarts, A.; Broekaart, D.W.M.; Mijnsbergen, C.; Jansen, F.E.; Van Hecke, W.; Spliet, W.G.M.; van Rijen, P.C.; Feucht, M.; Hainfellner, J.A.; Kršek, P.; Zamecnik, J.; Crino, P.B.; Kotulska, K.; Lagae, L.; Jansen, A.C.; Kwiatkowski, D.J.; Jozwiak, S.; Curatolo, P.; Mühlebner, A.; Lee, J.H.; Mills, J.D.; van Vliet, E.A.; Aronica, E.

DOI
10.1111/nan.12717

Publication date
2021

Document Version
Final published version

Published in
Neuropathology and Applied Neurobiology

Received: 18 October 2020 | Revised: 26 January 2021 | Accepted: 19 April 2021

DOI: 10.1111/nan.12717

Neuropathology and Applied Neurobiology WILEY

ORIGINAL ARTICLE

MicroRNA-34a activation in tuberous sclerosis complex during early brain development may lead to impaired corticogenesis

Anatoly Korotkov[1] | Nam Suk Sim[2] | Mark J. Luinenburg[1] | Jasper J. Anink[1] | Jackelien van Scheppingen[1,3] | Till S. Zimmer[1] | Anika Bongaarts[1] | Diede W. M. Broekaart[1] | Caroline Mijnsbergen[1] | Floor E. Jansen[4] | Wim Van Hecke[5] | Wim G. M. Spliet[5] | Peter C. van Rijen[6] | Martha Feucht[7] | Johannes A. Hainfellner[8] | Pavel Kršek[9] | Josef Zamecnik[10] | Peter B. Crino[11] | Katarzyna Kotulska[12] | Lieven Lagae[13] | Anna C. Jansen[14] | David J. Kwiatkowski[15] | Sergiusz Jozwiak[12,16] | Paolo Curatolo[17] | Angelika Mühlebner[1] | Jeong H. Lee[2,18] | James D. Mills[1,19,20] | Erwin A. van Vliet[1,21] | Eleonora Aronica[1,22]

[1]Department of (Neuro) Pathology, Amsterdam UMC, University of Amsterdam, Amsterdam Neuroscience, Amsterdam, The Netherlands

[2]Graduate School of Medical Science and Engineering, Korea Advanced Institute of Science and Technology, Daejeon, Republic of Korea

[3]Department of Neuroimmunology, Netherlands Institute for Neuroscience, Amsterdam, The Netherlands

[4]Department of Paediatric Neurology, University Medical Center Utrecht, Utrecht, The Netherlands

[5]Department of Pathology, University Medical Center Utrecht, Utrecht, The Netherlands

[6]University Medical Center, Brain Centre, Rudolf Magnus Institute for Neuroscience, Utrecht, The Netherlands

[7]Department of Pediatrics, Medical University Vienna, Vienna, Austria

[8]Institute of Neurology, Medical University Vienna, Vienna, Austria

[9]Department of Pediatric Neurology, 2nd Faculty of Medicine and Motol University Hospital, Prague, Czech Republic

[10]Department of Pathology and Molecular Medicine, 2nd Faculty of Medicine and Motol University Hospital, Prague, Czech Republic

[11]Department of Neurology, University of Maryland School of Medicine, Baltimore, MD, USA

[12]Department of Neurology and Epileptology, The Children's Memorial Health Institute, Warsaw, Poland

[13]Department of Development and Regeneration-Section Pediatric Neurology, University Hospitals KU Leuven, Leuven, Belgium

[14]Pediatric Neurology Unit, Universitair Ziekenhuis Brussel, Brussels, Belgium

[15]Brigham and Women's Hospital, Harvard Medical School, Boston, MA, USA

[16]Department of Child Neurology, Medical University of Warsaw, Warsaw, Poland

[17]Child Neurology and Psychiatry Unit, Systems Medicine Department, Tor Vergata University, Rome, Italy

[18]SoVarGen, Inc, Daejeon, Republic of Korea

[19]Department of Clinical and Experimental Epilepsy, University College London, London, UK

[20]Chalfont Centre for Epilepsy, Chalfont St Peter, UK

[21]Center for Neuroscience, Swammerdam Institute for Life Sciences, University of Amsterdam, Amsterdam, The Netherlands

[22]Stichting Epilepsie Instellingen Nederland, Heemstede, The Netherlands

Correspondence
Eleonora Aronica, Stichting Epilepsie Instellingen Nederland, Heemstede, The Netherlands.
Email: e.aronica@amsterdamumc.nl

Abstract

Aims: Tuberous sclerosis complex (TSC) is a genetic disorder associated with dysregulation of the mechanistic target of rapamycin complex 1 (mTORC1) signalling pathway.

Jeong H. Lee, James D. Mills, Erwin A. van Vliet, and Eleonora Aronica are joint senior authors.

Funding information
The research leading to these results has received funding from the European Union's Seventh Framework Program (FP7/2007-2013) under grant agreement 602102 (EPITARGET; EAvV, EA) and 602391 (EPISTOP; EA, MF, PK, KK, LL, ACJ, DJK, SJ, PC, AM, JDM, AM, JvS, FEJ), the European Union's Horizon 2020 Research and Innovation Programme under the Marie Sklodowska-Curie grant agreement 642881 (ECMED; AK, EA, EAvV) and 722053 (EU-GliaPhD; TSZ, EA, EAvV), as well as 952455 (EpiEpiNet, EA, EAvV, JM) and the Dutch Epilepsy Foundation, project number 20-02 (AM, MJL).

Neurodevelopmental disorders, frequently present in TSC, are linked to cortical tubers in the brain. We previously reported microRNA-34a (miR-34a) among the most upregulated miRs in tubers. Here, we characterised miR-34a expression in tubers with the focus on the early brain development and assessed the regulation of mTORC1 pathway and corticogenesis by miR-34a.

Methods: We analysed the expression of miR-34a in resected cortical tubers (n = 37) compared with autopsy-derived control tissue (n = 27). The effect of miR-34a overexpression on corticogenesis was assessed in mice at E18. The regulation of the mTORC1 pathway and the expression of the bioinformatically predicted target genes were assessed in primary astrocyte cultures from three patients with TSC and in SH-SY5Y cells following miR-34a transfection.

Results: The peak of miR-34a overexpression in tubers was observed during infancy, concomitant with the presence of pathological markers, particularly in giant cells and dysmorphic neurons. miR-34a was also strongly expressed in foetal TSC cortex. Overexpression of miR-34a in mouse embryos decreased the percentage of cells migrated to the cortical plate. The transfection of miR-34a mimic in TSC astrocytes negatively regulated mTORC1 and decreased the expression of the target genes RAS related (*RRAS*) and *NOTCH1*.

Conclusions: MicroRNA-34a is most highly overexpressed in tubers during foetal and early postnatal brain development. miR-34a can negatively regulate mTORC1; however, it may also contribute to abnormal corticogenesis in TSC.

KEYWORDS
mechanistic target of rapamycin, migration, miRNA, neurodevelopmental disorder, TSC

INTRODUCTION

Tuberous sclerosis complex (TSC) is a multisystem genetic disorder, associated with the development of multiple predominantly benign tumours in various organs [1]. Among the major histopathological manifestations of TSC in the brain are cerebral cortical malformations called tubers—lesions representing areas of distorted cellular architecture [1–3]. TSC pathology results from mutations in either one of the crucial negative regulators of the mechanistic target of rapamycin (mTOR), *TSC1* [4] or *TSC2* [5], causing a constitutive activation of mTOR kinase complex 1 (mTORC1) signalling pathway [6]. The normal functioning of the mTORC1 pathway is essential for proper neural development [7,8]. TSC is associated with early onset intractable epilepsy in 60%–90% of affected individuals, autism spectrum disorders (ASD), intellectual disability and neuropsychiatric disorders [9–13]. The pathological mechanisms leading to neurological manifestations of TSC are incompletely understood and remedies are often insufficient.

Our previous transcriptomic analysis of cortical tubers obtained from patients with TSC and intractable epilepsy revealed vast changes in the expression of protein-coding and non-coding genes associated with cell adhesion, immune response, neurogenesis and synaptic transmission [14,15]. MicroRNAs (miRs) are a class of small non-coding RNAs (18–22 nucleotides long) that regulate gene expression at the post-transcriptional level, which in mammals often leads to repressed target translation [16]. Aberrant expression of miRs can be associated with abnormal brain development and the pathogenesis of several neurodevelopmental diseases [17–19]. Previously, we identified the members of the miR-34 family (miR-34a, miR-34b and miR-34c) as the most overexpressed miR species in cortical tubers [15]. The miR-34 family has been implicated in the regulation of neurodevelopmental processes [15,20,21] and may be involved in abnormal corticogenesis in TSC, because cortical tubers are already present during embryonic brain development [22–24]. However, previous analyses of miR-34 expression have largely been restricted to the relatively late postnatal time points, which

Key Points

- MicroRNA-34a (MiR-34a) is overexpressed in cortical tubers from children with tuberous sclerosis complex with a peak during infancy
- MiR-34a negatively regulates constitutively activated mechanistic target of rapamycin complex 1 in human astrocytes
- MiR-34a overexpression impairs corticogenesis in the embryonic mouse brain, potentially through targeting genes involved in neuronal migration

do not reflect the period of potential neurodevelopmental pathological changes. We hypothesised that miR-34 overexpression in TSC could already be present during early brain development and could lead to disturbed corticogenesis, contributing to the neurologic manifestations of TSC.

In order to test this hypothesis, we analysed the expression of miR-34a in foetal and early postnatal TSC brain. We characterised the cell type-specific expression of miR-34a and the potential pathological mechanisms that may lead to miR-34a activation in an infant TSC brain. Furthermore, we studied the potential association between miR-34a and the mTORC1 pathway in vitro. Finally, the effect of miR-34a overexpression on corticogenesis was assessed in mouse embryos and in vitro.

MATERIALS AND METHODS

The extended version is available as Supporting Information.

Human samples

The brain tissue specimens included in this study were obtained from the archives of the department of Neuro (Pathology) of the Amsterdam University Medical Centers (Amsterdam UMC-Location AMC), the University Medical Center Utrecht, Motol University Hospital (Prague) and the Medical University Vienna. Postnatal TSC cortical samples were obtained from the patients who underwent resective surgery for the treatment of drug-resistant epilepsy (n = 38); postnatal control cortical samples were obtained from autopsies of patients without history of neurological diseases (n = 27) and foetal control samples were obtained following medically induced abortions (n = 15; Table 1). Foetal TSC cortical samples were obtained from the autopsies of foetuses diagnosed with TSC (n = 4; Table 2). All patients fulfilled the diagnostic criteria for TSC [25]. Brain tissue was either frozen and kept at −80°C (for molecular analysis) or fixed in 4% paraformaldehyde and embedded in paraffin (FFPE, for histological analysis). Informed consent was obtained for the use of brain tissue and for access to medical records for research purposes. Tissue was obtained and used in accordance with the Declaration of Helsinki and the Amsterdam UMC Research Code provided by the Medical Ethics Committee, and the study was approved by the local ethical committees of all participating medical centres.

Experimental animals

C57BL/6 mice (n = 3) were housed in isolator cages with food and water accessible ad libitum under a constant temperature of +23°C on a 12-h light-dark cycle (lights off at 7:00 PM). All procedures were approved by the Korea Advanced Institute of Science and Technology Institutional Animal Care and Use Committee.

In utero electroporation

In utero electroporation was performed as previously described [26,27]. Embryonic mice were electroporated at E14, and their brains were harvested after 4 days of development (at E18) and subsequently fixed in formalin, cryoprotected in 30% buffered sucrose and embedded in gelatine. Cryostat-cut sections (15 μm thick) were collected and placed on glass slides.

Plasmids

The miR-expressing plasmids were prepared by cloning the DNA fragments encoding for mature miR sequences flanked by ~100–200 bp regions into the pCIG (pCAG-MCS-IRES-eGFP) plasmid using EcoRI and SmaI restriction sites. MiR-34a was amplified from mouse genomic DNA. As a negative control, cel-miR-59 was amplified from the *Caenorhabditis elegans* genomic DNA. The primers used are listed in Table 3. The amplification was done using a high-fidelity DNA polymerase Immolase (Bioline). DNA extraction from agarose gel was done with NucleoSpin Gel and PCR Clean-up kit (Machinery-Nagel), and the plasmid DNA was isolated using NucleoBond PC100 Midi Kit (Machinery-Nagel). Sanger sequencing was used to confirm successful cloning. Validation of the mmu-mir-34a-expressing vector by transfection with polyethyleneimine showed increased expression of miR-34-5p in the mouse neuronal cell line HT-22 (median fold change [FC] =4.9, $p < 0.001$, Figure S8A) and in human HEK T293 cells (median FC =376, $p < 0.001$, Figure S8B).

Cell culture

Primary human astrocyte cultures were derived from the brains of three patients diagnosed with TSC and harbouring *TSC2* mutations (TSC astrocytes thereafter). Cells were treated with 100-nM rapamycin for 24 h and subsequently harvested for protein or RNA analysis. Human TSC astrocytes and the human SH-SY5Y neuroblastoma cell line were used for transfection experiments. The SH-SY5Y cells were not differentiated to resemble the phenotype of migrating neuronal progenitors. For miR-34a overexpression, cells were transfected with miR-34a-5p (ID: MC11030) or negative control (NC) mimic (cat. 4464059), (mirVana miRNA mimics; ThermoFisher Scientific). For miR-34a inhibition cells were transected with antagomiR against miR-34a-5p (cat. no. 4464084; assay ID: MH11030) and NC antagomiR (cat. no. 4464076). Oligonucleotides were delivered to the cells using Lipofectamine 2000 transfection reagent (Life Technologies) at a final concentration of 50 nM for a total of 48 h.

RNA isolation, reverse transcription and quantitative polymerase chain reaction

RNA isolation for miR analysis was done using the miRNeasy Mini kit (Qiagen Benelux) according to the manufacturer's instructions.

TABLE 1 Human samples

Surgical TSC samples

Sample *N*	Age (mon)	Gender	Used for	Region	Mutation
TSC1	7	f	RT-qPCR	fr	TSC2
TSC2	8	m	RT-qPCR/WB	fr	TSC1
TSC3	8	m	RT-qPCR	fr	TSC2
TSC4	8	m	RT-qPCR/WB	t/p	TSC2
TSC5	10	f	RT-qPCR	tp	TSC2
TSC6	11	f	RT-qPCR	tp	TSC1
TSC7	12	f	RT-qPCR	tp	TSC2
TSC8	12	m	RT-qPCR/WB	fr	TSC2
TSC9	23	m	RT-qPCR	fr	TSC2
TSC10	24	m	RT-qPCR/WB	fr	TSC2
TSC11	24	m	RT-qPCR/WB	fr	TSC2
TSC12	24	f	RT-qPCR/WB	tp	TSC2
TSC13	27	f	RT-qPCR	t/p	TSC1
TSC14	28	m	RT-qPCR	f/p	TSC2
TSC15	33	m	RT-qPCR	fr	TSC2
TSC16	37	m	RT-qPCR	tp	TSC2
TSC17	37	f	RT-qPCR/WB	tp	TSC2
TSC18	37	m	RT-qPCR/WB	fr	TSC2
TSC19	43	m	RT-qPCR	fr	TSC1
TSC20	48	m	WB	fr	TSC2
TSC21	49	f	RT-qPCR/WB	fr	TSC2
TSC22	67	m	RT-qPCR	fr	TSC2
TSC23	73	f	RT-qPCR	fr	TSC1
TSC24	97	m	RT-qPCR	fr	TSC1
TSC25	97	f	RT-qPCR	fr	TSC1
TSC26	99	f	RT-qPCR	fr	TSC2
TSC27	110	f	RT-qPCR	fr	TSC2
TSC28	121	f	RT-qPCR	fr	TSC2
TSC29	122	f	RT-qPCR	fr	TSC2
TSC30	122	m	RT-qPCR	fr	TSC2
TSC31	158	f	RT-qPCR	fr	TSC2
TSC32	195	m	RT-qPCR	fr	TSC2
TSC33	210	f	RT-qPCR	p	TSC1
TSC34	292	f	RT-qPCR	fr	TSC2
TSC35	365	m	RT-qPCR	fr	TSC2
TSC36	366	f	RT-qPCR	fr	TSC2
TSC37	368	f	RT-qPCR	tp	TSC1
TSC38	572	m	RT-qPCR	tp	TSC2

Fetal post-mortem control samples

Sample *N*	Age (GW)	Gender	Used for	Region
FET1	15	f	RT-qPCR	br
FET2	18	m	RT-qPCR	fr
FET3	20	m	RT-qPCR	br
FET4	21	f	RT-qPCR	ctx

(Continues)

TABLE 1 (Continued)

Fetal post-mortem control samples

Sample *N*	Age (GW)	Gender	Used for	Region
FET5	22	f	RT-qPCR	ctx
FET6	22	m	RT-qPCR	tp
FET7	22	m	RT-qPCR	ctx
FET8	22	m	RT-qPCR	tp
FET9	23	m	RT-qPCR	ctx
FET10	23	f	RT-qPCR	tp
FET11	23	f	RT-qPCR	tp
FET12	23	m	RT-qPCR	tp
FET13	25	m	RT-qPCR	tp
FET14	26	m	RT-qPCR	ctx
FET15	41	f	RT-qPCR	fr

Postnatal post-mortem control samples

Sample *N*	Age (mon)	Gender	Used for	Region
CTRL1	0	m	RT-qPCR/WB	fr
CTRL2	0	m	RT-qPCR	fr
CTRL3	1	m	RT-qPCR/WB	fr
CTRL4	2	f	RT-qPCR/WB	fr
CTRL5	2	f	RT-qPCR	tp
CTRL6	2	f	RT-qPCR	fr
CTRL7	3	f	RT-qPCR	tp
CTRL8	4	m	RT-qPCR/WB	fr
CTRL9	7	f	RT-qPCR/WB	ctx
CTRL10	12	f	RT-qPCR/WB	tp
CTRL11	24	f	RT-qPCR/WB	tp
CTRL12	37	m	RT-qPCR/WB	fr
CTRL13	49	f	RT-qPCR/WB	tp
CTRL14	85	f	RT-qPCR	fr
CTRL15	85	m	RT-qPCR	fr
CTRL16	122	m	RT-qPCR	fr
CTRL17	122	m	RT-qPCR	fr
CTRL18	158	m	RT-qPCR	fr
CTRL19	158	f	RT-qPCR	tp
CTRL20	183	m	RT-qPCR	fr
CTRL21	207	f	RT-qPCR	tp
CTRL23	304	f	RT-qPCR	ctx
CTRL24	377	m	RT-qPCR	ctx
CTRL25	377	m	RT-qPCR	ctx
CTRL26	475	f	RT-qPCR	fr
CTRL27	535	f	RT-qPCR	p

Note: In total, $n = 38$ surgical TSC samples were used (TaqMan RT-qPCR, $n = 37$ and western blot, WB, $n = 10$); $n = 15$ foetal autopsy control samples were used for RT-qPCR; and $n = 27$ postnatal autopsy control samples were used for RT-qPCR (RT-qPCR, $n = 27$) and western blot ($n = 9$).

Abbreviations: br, whole brain; ctx, cortex; f, female; f/p, fronto-parietal cortex; fr, frontal cortex; GW, gestational week; m, male; mon, months; RT-qPCR, reverse transcription-quantitative polymerase chain reaction; tp, temporal cortex; y, years.

TABLE 2 Human foetal samples used for histological analysis

Sample *N*	Age	Gender	Material	Used for	Region	Mutation
Foetal samples						
FET_TSC1	23 GW	m	Post-mortem	ISH	ctx	*TSC2*
FET_TSC2	27 GW	f	Post-mortem	ISH	fr	*TSC2*
FET_TSC3	32 GW	f	Post-mortem	ISH	fr	*TSC2*
FET_TSC4	34 GW	f	Post-mortem	ISH	fr	*TSC2*
FET_CTRL1	22 GW	m	Post-mortem	ISH	ctx	–
FET_CTRL3	28 GW	f	Post-mortem	ISH	fr	–
FET_CTRL4	31 GW	f	Post-mortem	ISH	fr	–
FET_CTRL5	35 GW	f	Post-mortem	ISH	fr	–
Postnatal samples						
PN_TSC1	8 months	m	Surgical	ISH/IHC	fr	*TSC2*
PN_CTRL1	5 months	m	Surgical	ISH/IHC	fr	–
PN_CTRL2	9 months	m	Surgical	ISH/IHC	fr	–

Note: Post-mortem samples obtained from autopsies of fetuses with TSC (n = 4) and control fetuses (n = 4) were used for in situ hybridisation method (ISH).

Abbreviations: ctx, cortex; f, female; fr, frontal cortex; GW, gestational week; m, male.

TABLE 3 List of oligonucleotides

RT-qPCR primers (human)

Gene symbol	Gene name	Forward	Reverse
AKT3	AKT Serine/Threonine Kinase 3	ATTATTGCAAAGGATGAAGTGGC	CGGTCTTTTGTCTGGAAGGA
C1ORF43	Chromosome 1 open reading frame 43	GATTTCCCTGGGTTTCCAGT	ATTCGACTCTCCAGGGTTCA
DAP2IP	DAB2 Interacting Protein	AAAAGGAGGAACCCAGACGC	TTTCTTGAGGCGACTCGTAGG
DCX	Doublecortin	TGGAGATGCTAACCTTGGGT	CAGAGACTGACAGTGGCTCCTAT
EF1a	Elongation factor 1 alpha	ATCCACCTTTGGGTCGCTTT	CCGCAACTGTCTGTCTCATATCAC
GAPDH	Glyceraldehyde 3-phosphate dehydrogenase	AGGCAACTAGGATGGTGTGG	TTGATTTTGGAGGGATCTCG
NOTCH1	Notch homolog 1, translocation-associated (Drosophila)	CTGCCTGTCTGAGGTCAATG	TCACAGTCGCACTTGTACCC
RAP1GAP	RAP1 GTPase activating protein	CAACACCGTGTCCACCAG	TTTCCCAGGAATAAGCAATGA
RELN	Reelin	TCGTCCTAGTAAGCACTCGC	TCGCCTAAGTGACCTTCGTC
RRAS	Related RAS viral (r-ras) oncogene homolog	GGCAGATCTGGAGTCACAGC	ACGTTGAGACGCAGTTTGG
RRAGC	Ras related GTP binding C	GGATTCTGCTCATGGGACTC	TGACATCTTATGAAACACCACCTT
RRAGD	Ras related GTP binding D	GGCTAGCGGACTACGGAGA	GGGGTCACTGAAGTCCAGAAC
SATB2	SATB Homeobox 2	GCACCAGAAGAAGACACCCTG	CAGGGACTGCTCACGGTCTG

Cloning primers

MiR	Forward	Reverse
hsa-miR-34a	TAAGCAGAATTCGCCTCTCCATC TTCCTGTGA	TGCTTACCCGGGCGTTGCTGAC CTCTGACCTT
cel-miR-59	TAAGCAGAATTCTACACATGGCG CCAATAAAA	TGCTTACCCGGGTTGAAAACTC TCGCTTACCG

In situ hybridisation probe

miR-34a-5p	5′DIG-AcaAccAgcTaaGacAcuGccA-DIG3′

Note: Oligonucleotide probe for ISH was designed against miR-34a-5p and had the following modifications: capital letters—locked nucleic acid (LNA) modifications, small letters—2-O-methyl modifications; DIG—digoxygenin label.

Abbreviations: ISH, in situ hybridisation method; RT-qPCR, reverse transcription-quantitative polymerase chain reaction

RNA isolation for mRNA analysis was done according to a conventional phenol–chloroform protocol. RNA was reverse-transcribed into cDNA using oligo-dT primers or specific primers for hsa-miR-34a-5p (assay no. 000426; ThermoFisher Scientific) and U6 small nuclear RNA (RNU6; assay no. 001973). The cDNA preparation and real-time quantitative polymerase chain reaction (qPCR) analysis were done as previously described [28]. The primers used for the reverse transcription (RT)-qPCR are listed in Table 3. The reactions were run on the Roche LightCycler 480 (Roche Applied Science) with a 384-multiwell format. Quantitation of data was performed using LinRegPCR software [29] as previously described [30].

Protein isolation and western blot analysis

Western blot analysis was done as previously described [28]. The primary and secondary antibodies are described in Table 4 (application WB). Chemiluminescent signal was detected using an ImageQuant LAS 4000 analyser (GE Healthcare) and the quantitative densitometric analysis was done using ImageJ software (U.S. National Institutes of Health).

In situ hybridisation

In situ hybridisation was done as previously described [28] with some modifications. The tissue sections were incubated with a probe against hsa-miR-34a-5p at a concentration of 100 nM for 1 h at 60°C. Nitro-blue tetrazolium chloride/5-bromo-4-chloro-3′-indolyphosphate *p*-toluidine salt or Vector Blue (#SK-5300; Vector Labs) were used as chromogenic substrates for alkaline-phosphatase detection.

The intensity of the miR-34a-5p in situ hybridisation signal (IHS) was analysed using ImageJ software [31] as optical density (OD) of a part of the image corresponding to different layers of the developing human cortex using 'Rodbard' function for calibration from mean grey value.

Immunohistochemistry

In situ hybridisation on human FFPE tissue was followed by immunohistochemical double-labelling and was performed as previously described [28]. The primary antibodies are described in Table 4 (application IHC). Afterwards, the sections were washed in phosphate-buffered saline (PBS) and incubated with the corresponding secondary antibodies using a polymer-based peroxidase immunocytochemistry detection kit (Brightvision plus kit; ImmunoLogic). The visualisation of the antibody-antigen binding was done using 3-amino-9-ethylcarbazole (Sigma-Aldrich).

Immunohistochemistry on mouse brain sections was done as previously described [26]. The primary and secondary fluorescent antibodies are described in Table 4. The ProLong Gold Antifade reagent with 4′,6-diamidino-2-phenylindole (ThermoFisher Scientific) was used to stain nuclei. The images were acquired using a Zeiss LSM510 confocal microscope.

Bioinformatic analysis

The target genes for miR-34a-5p were predicted using TargetScan [32]. The list of genes related to mTOR pathway regulation was constructed using the Gene Ontology (GO) categories 'neuron migration' (GO:0001764), 'regulation of cell migration' (GO:0030334), 'positive regulation of cell migration' (GO:0030335), 'negative regulation of cell migration' (GO:0030336), 'TOR complex' (GO:0038201) and 'positive regulation of TOR signalling' (GO:0032008). Hypergeometric testing was performed to assess the list for enrichment of 3′UTR targets, coding sequence or 5′UTR targets. Several target genes with the lowest total context++ scores, as given by TargetScan, were selected for RT-qPCR analysis. The gene interaction networks were built using STRING v11 online tool [33].

Statistical analysis

Statistical analyses were performed using Graphpad prism 5 (Graphpad Software). The Mann–Whitney *U*-test or the Kruskal–Wallis test with Dunn's post-hoc test was used for comparisons between groups. A value of $p < 0.05$ was assumed to indicate a significant difference.

RESULTS

Increased miR-34a expression in the cortical tubers during early postnatal development

The expression of miR-34a and miR-34b was evaluated in resected cortical tubers from patients with TSC ($n = 37$) in comparison with autopsy-derived cortical control samples ($n = 27$). TaqMan RT-qPCR analysis showed higher expression of miR-34a (median FC =3.4, $p < 0.001$; Figure 1A) and miR-34b (median FC =2.0, $p < 0.05$; Figure S1A) in TSC as compared with controls. The peak of miR-34a and miR-34b expression was observed during early years of life (0–4 years old, for miR-34a: median FC =17.5, $p < 0.001$; Figure 1B and for miR-34b: median FC =6.9, $p < 0.05$; Figure S1B). A similar trend was observed in the age group of 4–12 years old; however, the differences were not statistically significant (for miR-34a: median FC =2.9; Figure 1B and for miR-34b: median FC =3.1; Figure S1B). No difference between groups was observed in the age group older than 12 years (for miR-34a: median FC =1.1; Figure 1B and for miR-34b: median FC = −1.1; Figure S1B). The fold-change of expression was more significant for miR-34a than for miR-34b, and miR-34a was also expressed higher when compared with miR-34b (median FC =43.8, Figure S1C); therefore, we focused on miR-34a further on.

TABLE 4 List of antibodies

Antigen	Application	Catalog no., Vendor	Species	Clone	Dilution
Primary antibodies against human antigens					
B-actin	WB	MAB1501, Merck, Darmstadt, Germany	Ms	C4	1:30,000
Phospho-4E-BP1 (Thr37/46)	WB	#2855, Cell Signaling Technology (CST), Leiden, the Netherlands	Rb	236B4	1:1000
GFAP	IHC	Z0334, DAKO, Glostrup, Denmark	Rb	N/A	1:4000
Iba-1	IHC	019-19741, Wako Chemicals, Neuss, Germany	Rb	N/A	1:2000
JNK	WB	#9252, CST	Rb	N/A	1:1000
Phospho-JNK	WB/IHC	#9251, CST	Rb	N/A	1:1000/1:200
c-Myc	WB/IHC	#ab32, Abcam, Cambridge, UK	Ms	9E10	1:500/1:200
NeuN	IHC	#MAB377, Chemicon, Temecula, CA, USA	Ms	A60	1:2,000
P53	WB	#MA5-14067, ThermoFisher Scientific, Wilmington, DE, USA	Ms	DO-7 + TP53-12	1:500
P53	IHC	#M7001, DAKO	Ms	DO-7	1:100
S6	WB	#2217, CST	rb	5G10	1:1000
Phospho-S6 (Ser235/236)	WB/IHC	#4857, CST	Rb	91B2	1:1000/1:100
S6KB1	WB	#2708, CST	Rb	49D7	1:1000
Phospho-S6KB1 (Thr389)	WB	#9234, CST	Rb	108D2	1:1000
SMAD2/3	IHC	#3102, CST	Rb	N/A	1:1000
Phospho-SMAD2/3 (Ser465/467)	IHC	#8828, CST	Rb	D27F4	1:1,000
TMEM119	IHC	#HPA051870, Sigma-Aldrich, St. Louis, MO, USA	Rb	N/A	1:500
Other primary antibodies					
Cleaved Caspase-3 (Asp175)	IHC	#9661, CST	Rb	N/A	1:200
Cux-1 (mouse)	IHC	#sc13024, Santa Cruz, Dallas, USA	Rb	N/A	1:400
GFP	IHC	#AB1218, Abcam	Ms	9F9.F9	1:500
Digoxigenin	ISH	#11 333 089 001, Roche Applied Science, Basel, Switzerland	Sp	N/A	1:1500
Secondary antibodies					
Alexa Fluor 594-conjugated	IHC	#A11005, ThermoFisher Scientific	Gt	Ms	1:200
Alexa Fluor 488-conjugated	IHC	#A11008, ThermoFisher Scientific	Gt	Rb	1:200
Ig/HRP	WB	#P0448, DAKO	Gt	Rb	1:2500
Ig, human ads-HRP	WB	#1070-05, Southern Biotech, Birmingham, Alabama, US	Gt	Ms IgG1	1:2500
Ig, human ads-HRP	WB	#1080-05, Southern Biotech	Gt	Ms IgG2a	1:2500
Ig, human ads-HRP	WB	#1090-05, Southern Biotech	Gt	Ms IgG2b	1:2500

Abbreviations: Gt, goat; IHC, immunohistochemistry; ISH, in situ hybridisation method, Ms, mouse; N/A, not applicable; Rb, rabbit; Sp, sheep; WB, western blot.

MiR-34a is expressed in neuronal cells, astrocytes and giant cells

Histological characterisation of miR-34a expression by in situ hybridisation confirmed the RT-qPCR results. The IHS was observed in the grey matter (Figure 1C, Control) and the white matter (WM; Figure 1D, Control) in the infant (9 months old) autopsy control cortex. The IHS was stronger in the age-matched (8 months old) TSC brain cortex and was observed in the numerous cells with altered morphology characteristic of TSC (Figure 1C,D, TSC). Based on morphology and the presence of the neuronal marker NeuN, miR-34a IHS was detected in the control cortical neurons (Figure 1C, inset) and in dysmorphic neurons (DN) in TSC (Figure 1E, DN). Based on morphology and the presence of the astrocytic marker GFAP, miR-34a

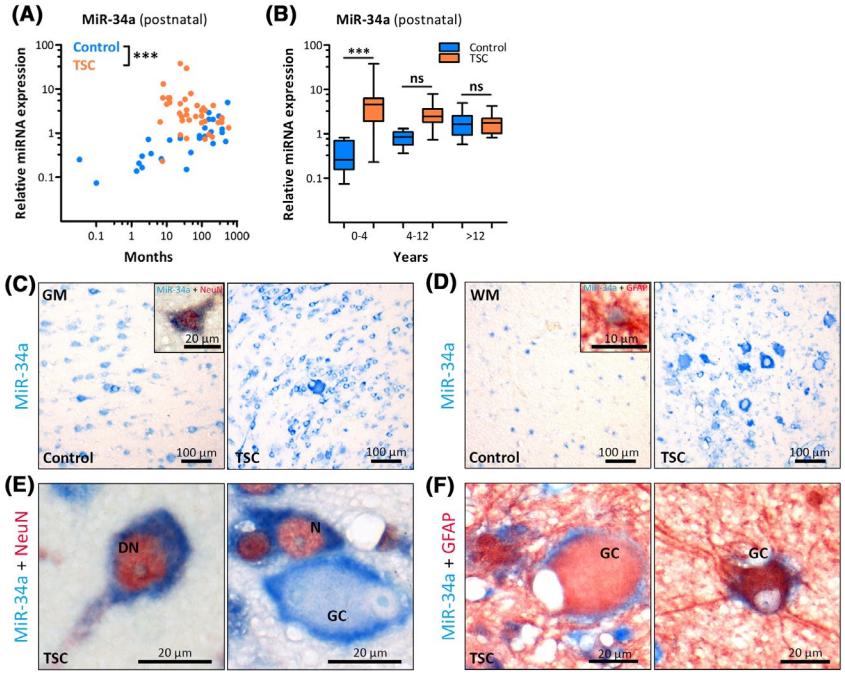

FIGURE 1 Increased miR-34a expression in cortical tubers during early postnatal development. (A, B) TaqMan RT-qPCR analysis: (A) miR-34a expression was higher (median FC =3.4, $p < 0.001$) in the resected cortical tubers from tuberous sclerosis complex (TSC) patients ($n = 37$) compared with autopsy-derived control tissue ($n = 27$); (B) MiR-34a was higher (FC =17.5, $p < 0.001$) in the TSC age group of 0–4 years old ($n = 19$) compared with the age-matched autopsy control group ($n = 13$), but did not differ significantly between TSC and age-matched controls at the ages 4–12 years old ($n = 10$ vs. $n = 5$) and >12 years old ($n = 8$ vs. $n = 9$); (C, D) MiR-34a-5p in situ hybridisation: infant TSC cortex (8 months old) compared with the autopsy-derived control cortex (9 months old) in the grey matter (C) and white matter (D); double-labelling of the miR-34a in situ hybridisation signal (IHS), shown in blue, with NeuN (C, inset) and GFAP (D, inset), shown in red; (E, F) Double-labelling showed co-localisation of miR-34a IHS with NeuN in normal and dysmorphic neurons (DN; E) and GFAP in giant cells (GC; E, F); ***$p < 0.001$; Mann–Whitney in (A) and Kruskal–Wallis with Dunn's post-hoc test in (B), median, error bars indicate min-max range.

IHS was detected in control WM astrocytes (Figure 1D, inset) and in giant cells (GC) in TSC (Figure 1E,F, GC). The miR-34a IHS was not co-localised with the markers of microglia Iba-1 (Figure S2A) or TMEM119 (Figure S2B) in either TSC or control tissue.

Activators of miR-34a are overexpressed in cortical tubers

We further analysed the markers of signalling pathways known to activate miR-34a expression. Western blot analysis of the resected cortical tubers from 0 to 4 years old patients ($n = 7$ TSC; $n = 8$ controls) demonstrated increased expression of the mTORC1 activation marker p-4E-BP1 (median FC =22.0, $p < 0.05$), the tumour-suppressor protein p53 (median FC =7.6, $p < 0.001$), oncogene c-Myc (median FC =29.5, $p < 0.05$) and p-JNK (median FC =5.1, $p < 0.01$; Figure 2A,B). Weak expression in the control cortex, but stronger expression in tubers, was observed for p-S6 (Figure 2C), p53 (Figure 2D), c-Myc (Figure 2E) and p-JNK (Figure 2F). Double-labelling of miR-34a with these markers in GC and DN revealed a spectrum of various phenotypes, including co-localisation of both miR-34a and each marker, as well as expression of either miR-34a or a marker (indicated by +/− signs in Figure 2C–F). The expression of p53 showed nuclear localisation (Figure 2D, arrowhead). P-JNK in tubers was expressed by cells with astrocytic morphology (Figure 2E, far-right panel). Additionally, the expression of p-SMAD2/3 was ubiquitously present in the cell nuclei in TSC in cells with miR-34a IHS, whereas only some cells expressed it in control brain (Figure S3).

MiR-34a negatively regulates mTORC1

The relationship between miR-34a and mTORC1 pathway was assessed in primary human astrocytes obtained from patients with TSC. Firstly, we tested the hypothesis that mTORC1 pathway may regulate miR-34a expression by treating astrocytes with rapamycin. Rapamycin effectively inhibited the mTORC1 pathway (Figure 3A) as evidenced by the reduced phosphorylation of S6 ($p < 0.001$; Figure 3B) and S6KB1 ($p < 0.001$; Figure S4A). The expression of miR-34a was slightly higher following rapamycin treatment (mean FC =1.3, $n = 3$, $p < 0.05$; Figure 3C).

We next investigated the effect of miR-34a overexpression or inhibition on mTORC1 pathway in TSC astrocytes. Transfection of astrocytes with miR-34a mimic resulted in increased expression of miR-34a (median FC =3163, $p < 0.001$; Figure S4B) and transfection with miR-34a antagomiR resulted in decreased expression of miR-34a (median FC = −4.2, $p < 0.001$, Figure S4C). The phosphorylation of S6

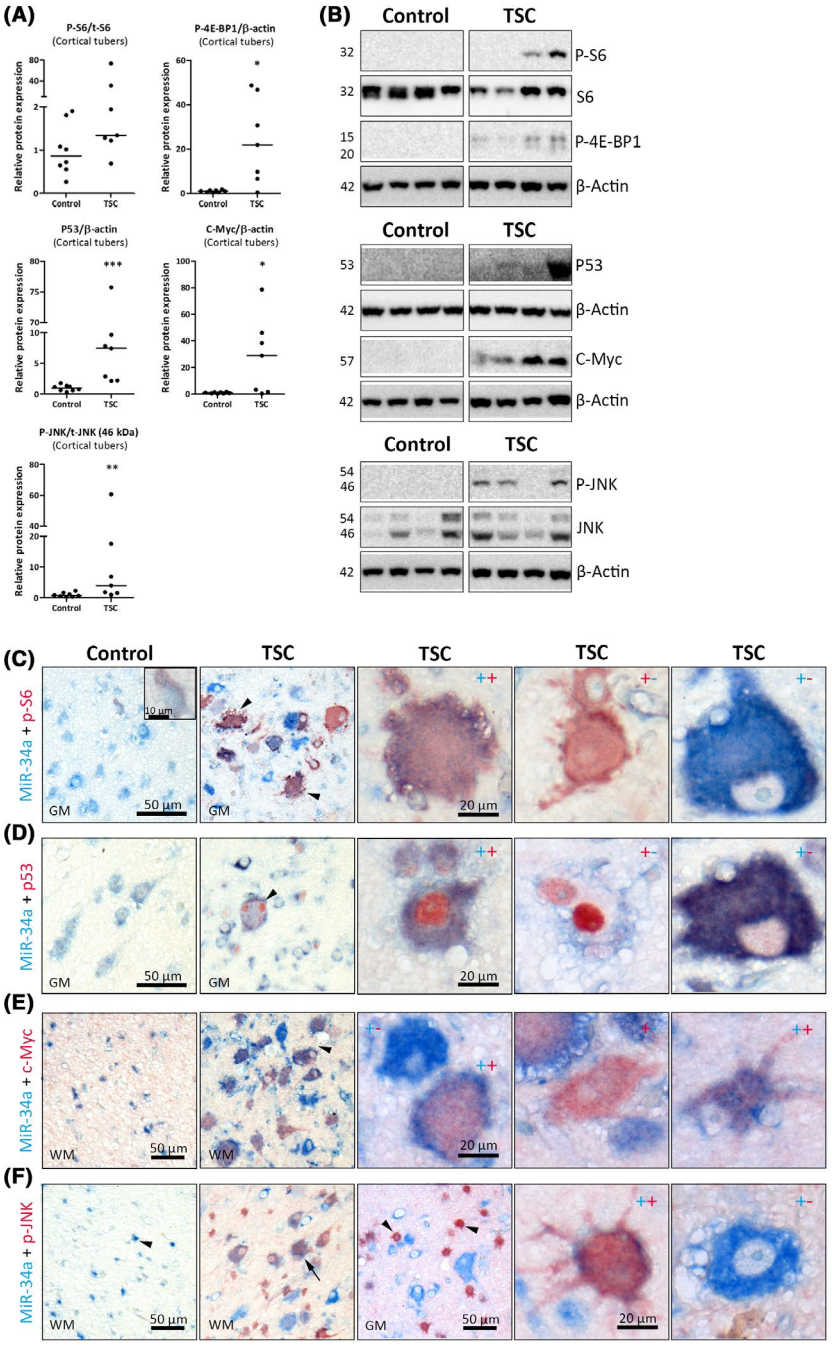

FIGURE 2 Increased expression of miR-34a-activating pathways in cortical tubers. (A) Relative protein expression of pathological markers in cortical tubers compared with autopsy-derived controls; (B) representative western blots; (C–F) in situ hybridisation with double-labelling: (C) P-S6 was expressed by giant cells (arrowheads) and co-localised with miR-34a in situ hybridisation signal (IHS) to various extent; (D) expression of p53 with nuclear localisation in giant cells co-localised with miR-34a IHS (arrowhead); (E) expression of c-Myc co-localised with miR-34a IHS (arrowhead); (F) expression of p-JNK in control white matter (arrowhead), in giant cells in tuberous sclerosis complex (TSC) white matter (arrow), as well as in astrocytes in TSC grey matter (arrowheads); blue +/− sign indicate miR-34a IHS presence; red +/− indicate maker expression presence; scale bar in each panel is as indicated at the closest panel to the left, WM, white matter, GM, grey matter

was reduced following transfection of miR-34a (mean FC = −1.7, n = 3, p < 0.001; Figure 3D,E) as compared with the negative control. The inhibition of miR-34a by antagomiR did not change the phosphorylation of S6 (Figure 3E). Bioinformatical analysis showed the enrichment of genes associated with mTORC1 pathway regulation among the potential targets of miR-34a (hypergeometric test, p < 0.001 for targets in 3′UTR, 5′UTR and the coding region). We analysed significantly enriched target genes (Figure S4D), including *RRAGC*, *RRAGD*, *RRAS*, *RAP1GAP* and *AKT3* and assessed their expression following miR-34a overexpression (Figure 3F). The expression of *RRAS* was reduced following miR-34a overexpression in astrocytes (mean FC = −2.5, n = 3, p < 0.001; Figure 3G) and in neuroblastoma cell line SH-SY5Y (mean FC = −1.7, p < 0.001; Figure S4E), as expected from the presence of a miR-34a target site in the *RRAS* 3′UTR (Figure S4F). The inhibition of miR-34a in TSC astrocytes resulted in slightly upregulated expression of *RRAS* (mean FC =1.2, n = 3, Figure 3G).

Increased miR-34a expression in the cortical tubers in the human foetal brain

The RT-qPCR analysis in the control tissue showed that post-natal miR-34a expression was higher compared with foetal expression (median FC =9.8, p < 0.01; Figure S5). In the foetal cortex, variable miR-34a IHS was observed in TSC and controls depending on the layer of cortex and age (Figure S6). A higher IHS in all layers of cortex was

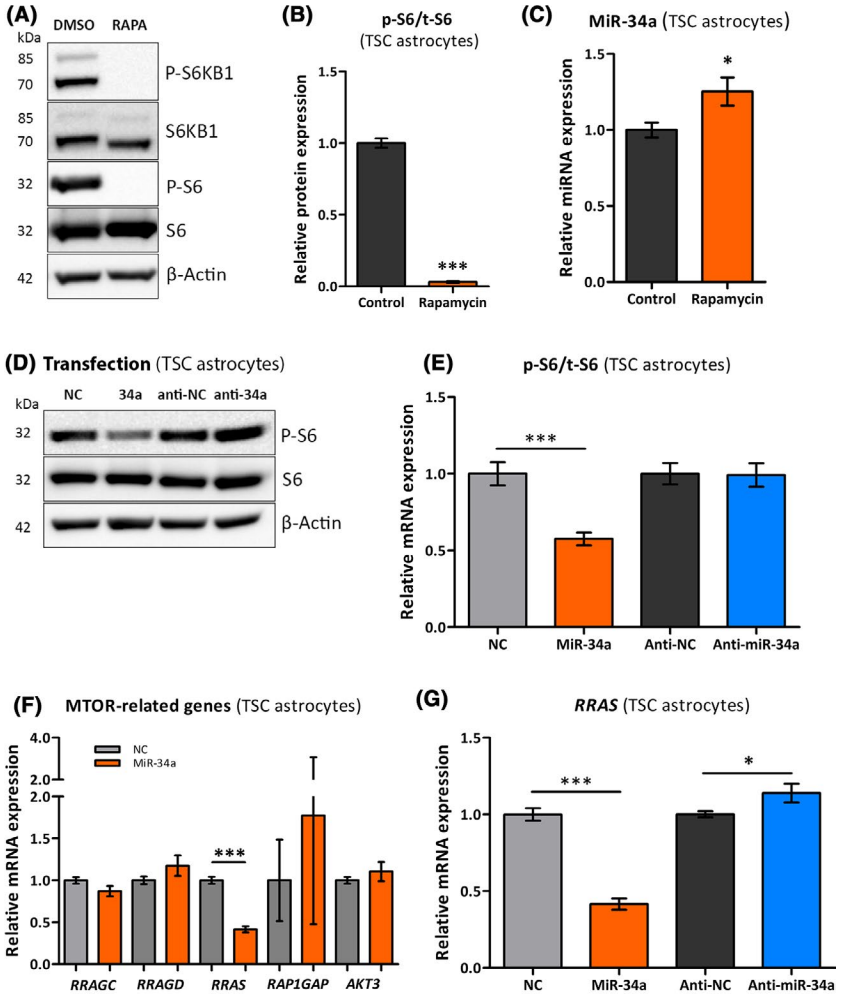

FIGURE 3 MiR-34a negatively regulates mechanistic target of rapamycin complex 1 (mTORC1) in human tuberous sclerosis complex (TSC) astrocytes. (A) Western blot analysis of mTORC1 markers in human TSC astrocytes treated with rapamycin (100 nM) for 24 h; (B) inhibition of mTORC1 pathway confirmed by the decreased ratio of phospho-S6 (p-S6) to total S6 (t-S6) after rapamycin treatment compared with control (0.05% DMSO); (C) TaqMan RT-qPCR analysis for miR-34a expression in astrocytes following rapamycin treatment; (D) western blot analysis for p-S6 expression in human TSC astrocytes transfected with miR-34a mimic or antagomiR; (E) quantification of western blot showed a decreased p-S6 to t-S6 ($p < 0.001$) after miR-34a overexpression compared with the negative control (NC); (F) RT-qPCR analysis of the miR-34a target gene expression in TSC astrocytes following miR-34a overexpression; (G) RT-qPCR analysis for a miR-34a target *RRAS* in TSC astrocytes following miR-34a overexpression or inhibition by antagomiR (anti-miR-34a); $^{*}p < 0.05$, $^{***}p < 0.001$; Mann–Whitney in (B), (C), (E), (G) and Kruskal–Wallis with Dunn's post-hoc test in (F); error bars indicate standard error of mean

observed in TSC at the gestational week (GW) 27 as compared with the age-matched control at GW 28 (Figure 4A–D). Moderate miR-34a IHS was observed in the cells of the upper-layer cortical plate (CP UL; Figure 4A) and subplate (SP), with the strongly-expressing cells observed in TSC (Figure 4B, arrows). Moderate IHS was observed in cells with the morphology of migrating neural progenitor cells, and strong IHS was observed in GC in the intermediate zone (IZ; Figure 4C). Moderate IHS was observed in the subventricular zone (SVZ) with strongly-expressing cells and disorganised cellular architecture present in TSC (Figure 4D). The miR-34a IHS relative OD measured in all samples ($n = 4$ foetal TSC, $n = 4$ foetal control) was higher in the SP (median FC = 1.5, $p < 0.05$; Figure 4E) and in the IZ (median FC = 2.1, $p < 0.05$; Figure 4E) as compared between TSC and controls.

Bioinformatic analysis showed an enrichment of genes associated with neuronal migration among the potential targets of miR-34a (hypergeometric test, $p < 0.001$ for targets in 3′UTR, 5′UTR and the coding region). We analysed significantly enriched target genes (Figure S7A), including *DCX*, *SATB2*, *RELN*, *DAP2IP* and *NOTCH1* and analysed their expression in SH-SY5Y neuroblastoma cell line following miR-34a overexpression using RT-qPCR (Figure 4F). The expression of *NOTCH1* was lower following miR-34a overexpression in SH-SY5Y (mean FC = −1.4, $p < 0.01$; Figure 4G), as expected from the presence of a miR-34a target site in the *NOTCH1* 3′UTR (Figure S7B). The expression of *NOTCH1* was also lower following miR-34a overexpression in TSC astrocytes (mean FC = −1.25, $p < 0.01$; $n = 3$), whereas miR-34a inhibition by antagomiR resulted

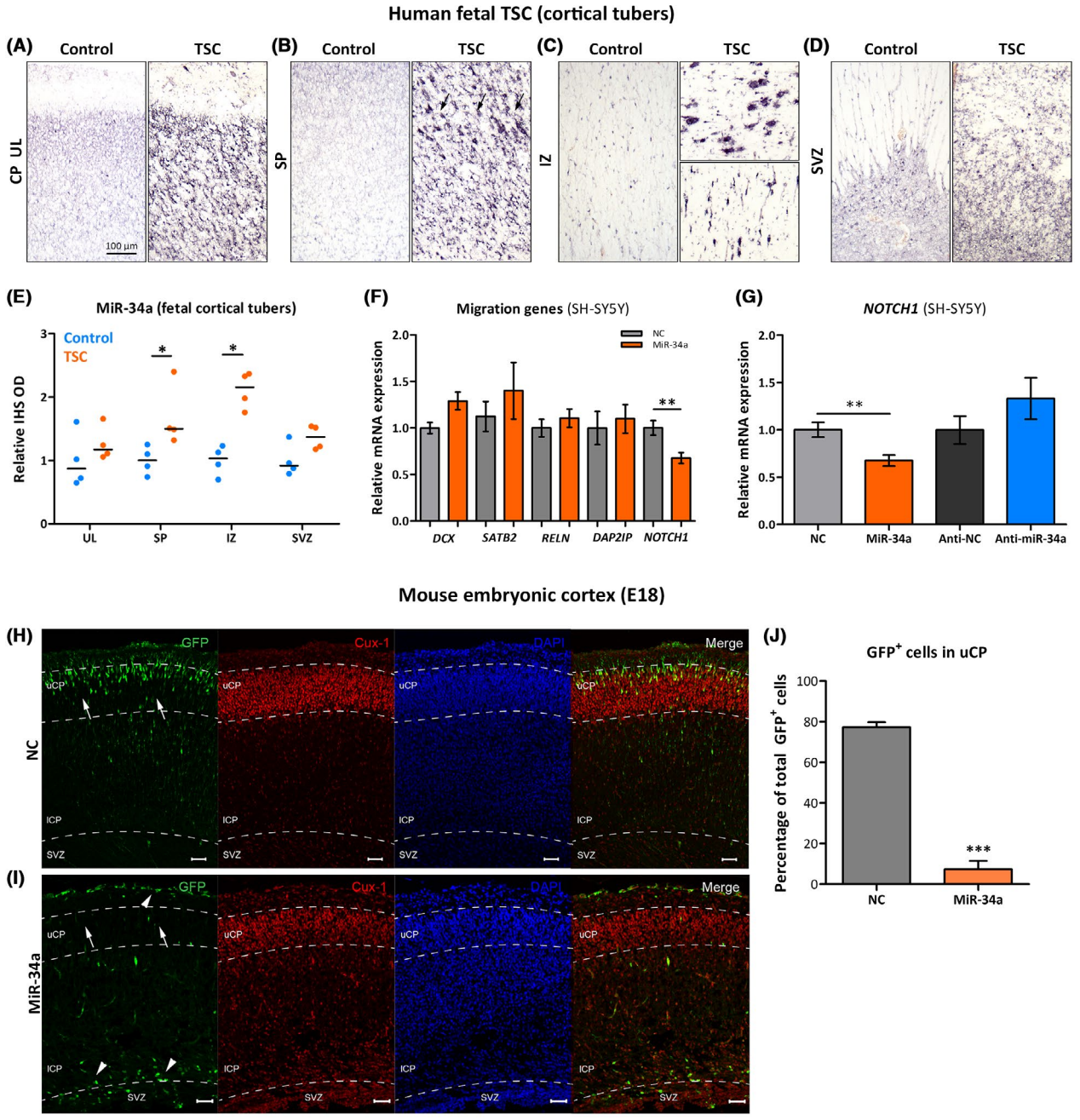

FIGURE 4 MiR-34a overexpression affects corticogenesis during foetal brain development. (A–D) In situ hybridisation in human foetal autopsy-derived brain cortex: tuberous sclerosis complex (TSC) (27 gestational week [GW]) vs. control (28 GW); (A) higher miR-34a in situ hybridisation signal (IHS) was seen in the upper layers (UL) of cortical plate (CP) and (B) subplate (SP, arrows indicate cells with strong miR-34a IHS not observed in control); (C) strong miR-34a IHS was observed in giant cells and migrating neural progenitors in the intermediate zone (IZ); (D) MiR-34a IHS was present in the subventricular zone (SVZ) in both TSC and control; (E) quantification of relative OD of the miR-34a IHS in foetal TSC (n = 4) and controls (n = 4); (F, G) RT-qPCR analysis: (F) expression of miR-34a target genes involved in migration following miR-34a mimic transfection; (G) RT-qPCR analysis of the miR-34a target gene *NOTCH1* in SH-SY5Y cells following transfection with miR-34a mimic or antagomiR (anti-miR-34a); (H, I) Immunohistochemistry for GFP and Cux-1 in the mouse cortex at E18: GFP immunoreactivity was mostly observed in the upper CP (uCP) after transfection with the negative control plasmid (NC) and co-localised with Cux-1 (merge panel); GFP immunoreactivity was observed in the SVZ, lower CP (lCP) and marginal zone, but was almost absent in the uCP after transfection with miR-34a-overexpressing plasmid; (J) the percentage of GFP-positive cells located in the uCP was 7% (4 of 44, n = 3) for miR-34a, which was lower ($p < 0.001$) than in the NC group (77%, 135 of 174, n = 3); arrows indicate the uCP; arrowheads indicate aberrantly migrated cells; ***$p < 0.001$; Mann–Whitney U-test; error bars indicate standard error of mean; scale bar—100 µm

in higher *NOTCH1* expression in TSC astrocytes (mean FC =1.3, $p < 0.05$; $n = 3$, Figure S7C).

Overexpression of miR-34a affects migration during mouse embryonic brain development

Next, we overexpressed miR-34a with a pCIG-mmu-mir-34a-eGFP vector in mouse embryos by in utero electroporation at E14. The expression of GFP was assessed at E18, and the majority of GFP-positive cells expressing negative control vector were located in the upper layer of the cortical plate (uCP) and co-localised with the marker of upper-layer neurons Cut Like Homeobox 1 (Cux1; Figure 4H). In contrast, the majority of GFP-positive cells overexpressing miR-34a were not located in the upper layers of the cortical plate but were rather split in two clusters: the first located in the SVZ and the lower part of the cortical plate and the second located in the marginal zone (Figure 4I, arrowheads). Quantitative analysis showed a lower percentage of GFP-positive cells located in the upper layers of the cortical plate for miR-34a overexpressing-condition compared with the negative control condition (7% vs. 77%, $p < 0.001$, $n = 3$; Figure 4J). Immunohistochemical analysis of the expression of cleaved caspase-3 did not reveal more apoptotic cell death in the cells overexpressing miR-34a compared with the negative control (Figure S9A,B).

DISCUSSION

We investigated the expression of miR-34a in resected cortical tubers from TSC patients and found increased miR-34a expression, particularly in young children and foetuses. MiR-34a overexpression during infancy in TSC was concomitant with the pathological activation of signalling pathways, including mTORC1, p53, c-Myc and JNK. Overexpression of miR-34a inhibited mTORC1 activation in human astrocytes derived from patients with TSC. However, overexpression of miR-34a in the mouse embryonic brain resulted in disrupted corticogenesis, which may depend on the regulation of genes involved in neuronal migration, such as *RRAS* and *NOTCH1*.

Increased expression of miR-34a in cortical tubers: Focus on the early development

We previously identified miR-34 family members among the most upregulated miRs in the tissue resected from brains of TSC patients, including cortical tubers [15] and subependymal giant cell astrocytomas [34]. As a follow-up study, we focused on miR-34a, because miR-34a is the most highly expressed miR of its family in the brain and one of the most abundantly expressed miRs in the adult brain overall [35,36]. Dombkowski et al. previously reported increased miR-34a expression in cortical tubers and pointed out the importance of considering the age of subjects when assessing miR-34a expression [37]. Indeed, our analysis showed a dramatic increase in miR-34a expression as early as Week 23 of gestation and during infancy. In the normal brain, where neurons are the primary contributors to the overall miR-34a level, total miR-34a expression gradually increases with advancing age. However, in TSC the presence of abnormal cells, which highly express miR-34a in tubers, such as GC, DN and reactive astrocytes, results in an early peak in miR-34a expression. This dramatic increase becomes less obvious as normal neurons mature and their contribution to overall miR-34a increases. In addition, cortical tubers of all subtypes demonstrate lower density of neurons compared with control cortex [3]. These observations may explain why the difference in miR-34a expression becomes less pronounced when compared between groups of older subjects.

MiR-34a has been previously implicated in several processes associated with brain development, such as epithelial-mesenchymal transition, apoptosis, neuron differentiation, migration and neurite outgrowth [20,21,35,38–41]. Moreover, miR-34a overexpression in TSC has been predicted to regulate a network of genes involved in glutamatergic neurotransmission, crucial for neural development [15]. Therefore, the overexpression of miR-34a may have a negative impact on the proper neural development and contribute to aberrant corticogenesis in TSC.

MiR-34a negatively regulates mTORC1

The increase in miR-34a is likely to be secondary to the activation of pathological pathways in cortical tubers. Constitutive activation of the mTORC1 plays a central role in TSC pathology [1]. MiR-34a is able to inhibit mTORC1, as shown in astrocytes from TSC patients. GC and DN display the markers of mTORC1 activation [22,42] and also highly express miR-34a, thus miR-34a increase in tubers may have a compensatory nature. The activation of mTORC1 itself is unlikely to be the direct cause of miR-34a overexpression, because the inhibition of mTORC1 signalling did not lead to a decrease in miR-34a expression. Several other pathological pathways may be responsible for the direct activation of miR-34a as well. The miR-34 family members have tumour-suppressor functions and can be transcriptionally regulated by p53 protein [43–47]. The constitutive activation of mTORC1 leads to the accumulation of phosphorylated p53 [48–50], and a loss of a single allele of *TSC2* can be enough for p53 activation [51]. GC and DN with activated p53, indeed, express miR-34a; however, a wide spectrum of other cellular phenotypes includes cells with high miR-34a and low p53, and vice versa. Moreover, not all of the investigated tuber samples show high expression of p53. These observations indicate that the overexpression of miR-34a in tubers cannot be solely explained by p53 activation. Several miR-34a-activating signalling pathways independent of p53 have also been described [52]. Accordingly, the expression of miR-34a is evident in the cells with the activated oncogene c-Myc, as well as JNK and TGF-β1 pathways. Interestingly, the activation of JNK pathway is observed in the cells with astroglial morphology; therefore JNK

may specifically mediate astrocytic activation in tubers. Activated astrocytes further contribute to the chronic inflammation in TSC brain [3,14,15,53,54]. These and other pathways may be responsible for miR-34a activation, which in turn provides a negative regulation to mTORC1, the primary driver of the TSC pathology.

Increased miR-34a affects corticogenesis in foetal brain

Overexpression of miR-34a in the cortical tubers from foetuses with TSC indicates that it may already have an impact on proper corticogenesis during embryonic development. Cortical tubers, mainly featuring GC, but yet devoid of DN, are estimated to appear as early as at 10–20 weeks of gestation in the developing TSC brain [22–24,55–59]. The associated increase in miR-34a may inhibit the constitutively activated mTORC1. Therefore, the primary effect of increased miR-34a is beneficial to alleviate the pathology, because dysregulated mTORC1 in the developing cortex is associated with the pathogenesis of neurological disorders, such as epilepsy, ASD and mental disability [6,56,57].

However, the prematurely high levels of miR-34a may also lead to aberrant regulation of the processes essential for corticogenesis. Although GC were the most conspicuous cell in terms of miR-34a expression, other cells in the foetal TSC brain strongly express miR-34a as well, such as migrating neuroblasts and neurons of the cortical plate. It is evident that the overexpression of miR-34a alone in the normal mouse embryonic cortex exerts a disrupting effect on corticogenesis. This could be explained by the disturbed migration of neural progenitor cells. Bioinformatic analysis supports this hypothesis, because miR-34a is estimated to target a network of genes involved in neuronal migration. This includes a gene encoding for the protein upstream of the mTORC1—Ras-related (RRAS), which was downregulated following miR-34a overexpression in our experiments. RRAS is a small GTPase, which is involved in actin cytoskeleton organisation through the modulation of integrin 1 alpha activity [60], and its inhibition has been shown to prevent cell migration, the effect mediated by phosphoinositide 3-kinase [61], which is deregulated in TSC. However, despite the observed strong effects on *RRAS* in human astrocytes, further experiments, such as a luciferase reporter assay, and target site knockout should be performed to confirm whether the regulation of this novel miR-34a target is through a direct or indirect interaction with miR-34a. Another important gene downregulated by miR-34a in our analysis was *NOTCH1*, a previously validated target of miR-34a [62]. NOTCH1 signalling has been shown to influence various stages of neurogenesis from differentiation of radial glial-like neural stem cells to synapse development of mature neurons [63,64]. Previously, the effect of miR-34a on the NOTCH1 signalling was shown in murine neural progenitor cells [40]. The increased miR-34a in TSC may influence the pleotropic action of NOTCH1 signalling on neural development.

Other potential mechanisms by which miR-34a affects corticogenesis have been proposed as well. The overexpression of miR-34a has been previously shown to inhibit the motility of human neural progenitor cells [65], and the overexpression of miR-34a in mice led to a decreased migration of neuroblasts, potentially through the reduction of the miR-34a target doublecortin [39]. It is important to mention that the decreased number of cells in the cortical plate of mice following miR-34a overexpression may indicate that the migration is delayed, rather than abolished; therefore, other time points should be assessed. However, overall, there is plentiful evidence that the increased miR-34a by itself could cause a disturbance in corticogenesis. This, in combination with previously published observations, provide substantial mechanistic basis for miR-34a contribution to the pathogenesis of neurological abnormalities observed in TSC.

Inhibition of miR-34a as therapeutic approach against neurological abnormalities in TSC

The inhibition of miR-34 family members can cause developmental defects [66,67]. However, we showed that increased expression of miR-34a in TSC can also cause defects in corticogenesis. Normalisation of the miR-34a level with miR-34a inhibitors could be explored as a novel therapy against neurological abnormalities in TSC. These inhibitory approaches can have multiple forms, including stable and specific chemically modified oligonucleotides, such as specific LNA probes [68], miRNA sponges [69] and RNA zipper molecules [70] delivered using nanoparticles or adeno-associated viruses [71]. Although care should be taken due to the role of miR-34a as tumour suppressor, which is often lost in oncological malignancies [72], thus, a time-limited treatment should be considered. Because the increase in miR-34a was most evident during early brain development, the therapeutic intervention would be most efficient in utero and during infancy. Inhibitors of mTORC1 have also been shown efficacious in reduction of neurological manifestations of TSC, such as the frequency of spontaneous seizures [73,74]. The inhibition of mTORC1 by rapamycin did not strongly affect miR-34a in TSC astrocytes and the use of antagomiR to block miR-34a did not affect mTORC1. Therefore, the potential therapeutic effects of these two interventions could be combined to achieve synergistic effect. The studies are warranted in animal TSC models to study the possibility of using miR-34a inhibition as an adjuvant therapy to mTORC1 inhibition.

CONCLUSIONS

MicroRNA-34a is overexpressed in cortical tubers during foetal and early postnatal brain development of TSC patients and may be involved in the inhibition of the constitutively activated mTORC1. However, the increased expression of miR-34a in the developing brain may lead to disturbed corticogenesis, potentially affecting neuronal migration. Whether the increased expression of miR-34a contributes to the complex and variable

clinical phenotypes encountered in TSC patients deserves further investigation.

ETHICS STATEMENT

All procedures performed in the study were in accordance with the ethical standards of the participating research centres.

ACKNOWLEDGEMENTS

The research leading to these results has received funding from the European Union's Seventh

Framework Program (FP7/2007-2013) under grant agreement 602102 (EPITARGET; EAvV, EA) and

602391 (EPISTOP; EA, MF, PK, KK, LL, ACJ, DJK, SJ, PC, AM, JDM, AM, JvS, FEJ), the European Union's

Horizon 2020 Research and Innovation Programme under the Marie Sklodowska-Curie grant

agreement no. 642881 (ECMED; AK, EA, EAvV) and no. 722053 (EU-GliaPhD; TSZ, EA, EAvV), as well as

no. 952455 (EpiEpiNet, EA, EAvV, JM) and the Dutch Epilepsy Foundation, project number 20-02 (AM,MJL).

CONFLICT OF INTEREST

J. H. Lee is a co-founder and CTO of SoVarGen, Inc., which seeks to develop new diagnostics and therapeutics for brain disorders. The remaining authors have no conflicts of interest to report. We confirm that we have read the Journal's position on issues involved in ethical publication and affirm that this report is consistent with those guidelines.

AUTHOR CONTRIBUTION

Anatoly Korotkov, Nam Suk Sim, J. H. Lee, James D. Mills, Erwin A. van Vliet and Eleonora Aronica conceived and designed the analysis. Mark J. Luinenburg, Jasper J. Anink, Jackelien van Scheppingen, Till S. Zimmer, Anika Bongaarts, Diede W. M. Broekaart and Caroline Mijnsbergen contributed to selection and preparation of material and helped with experimental work and methodology. Floor E. Jansen, Wim Van Hecke, Wim G. M. Spliet, Peter C. van Rijen, Martha Feucht, Johannes A. Hainfellner, Pavel Kršek, Josef Zamecnik, Peter B. Crino, Katarzyna Kotulska, Lieven Lagae, Anna C. Jansen, David J. Kwiatkowski, Sergiusz Jozwiak, Paolo Curatolo, and Angelika Mühlebner provided human patient tissue and clinical data. Anatoly Korotkov, Nam Suk Sim and James D. Mills analysed the data. Erwin A. van Vliet, James D. Mills, J. H. Lee and Eleonora Aronica contributed to the data interpretation and writing of the manuscript. All authors discussed the results and contributed to the final manuscript.

PEER REVIEW

The peer review history for this article is available at https://publons.com/publon/10.1111/nan.12717.

DATA AVAILABILITY STATEMENT

The data that support the findings of this study are available from the corresponding author upon reasonable request.

ORCID

Anatoly Korotkov https://orcid.org/0000-0002-8313-6282
Till S. Zimmer https://orcid.org/0000-0002-6869-3697
Anika Bongaarts https://orcid.org/0000-0003-1451-4240
Diede W. M. Broekaart https://orcid.org/0000-0002-4842-0659
Peter B. Crino https://orcid.org/0000-0002-6232-3740
Katarzyna Kotulska https://orcid.org/0000-0002-5015-250X
Lieven Lagae https://orcid.org/0000-0002-7118-0139
Anna C. Jansen https://orcid.org/0000-0002-3835-2824
David J. Kwiatkowski https://orcid.org/0000-0002-5668-5219
Sergiusz Jozwiak https://orcid.org/0000-0003-3350-6326
Angelika Mühlebner https://orcid.org/0000-0001-9102-7353
Jeong H. Lee https://orcid.org/0000-0002-2299-630X
James D. Mills https://orcid.org/0000-0002-9910-2933
Erwin A. van Vliet https://orcid.org/0000-0001-5747-3202
Eleonora Aronica https://orcid.org/0000-0002-3542-3770

REFERENCES

1. Curatolo P, Moavero R, van Scheppingen J, Aronica E. mTOR dysregulation and tuberous sclerosis-related epilepsy. *Expert Rev Neurother*. 2018;18(3):185-201.
2. Crino PB. Evolving neurobiology of tuberous sclerosis complex. *Acta Neuropathol*. 2013;125(3):317-332.
3. Mühlebner A, van Scheppingen J, Hulshof HM, et al. Novel histopathological patterns in cortical tubers of epilepsy surgery patients with tuberous sclerosis complex. *PLoS One*. 2016;11(6):e0157396.
4. van Slegtenhorst M, de Hoogt R, Hermans C, et al. Identification of the tuberous sclerosis gene TSC1 on chromosome 9q34. *Science*. 1997;277(5327):805-808.
5. European Chromosome 16 Tuberous Sclerosis Consortium. Identification and characterization of the tuberous sclerosis gene on chromosome 16. *Cell*. 1993;75(7):1305-1315.
6. Crino PB. mTOR signaling in epilepsy: insights from malformations of cortical development. *Cold Spring Harb Perspect Med*. 2015;5(4):a022442.
7. Saxton RA, Sabatini DM. mTOR signaling in growth, metabolism, and disease. *Cell*. 2017;168(6):960-976.
8. Lipton JO, Sahin M. The neurology of mTOR. *Neuron*. 2014;84(2):275-291.
9. Curatolo P, Nabbout R, Lagae L, et al. Management of epilepsy associated with tuberous sclerosis complex: updated clinical recommendations. *Eur J Paediatr Neurol*. 2018;22(5):738-748.
10. Bolton PF. Neuroepileptic correlates of autistic symptomatology in tuberous sclerosis. *Ment Retard Dev Disabil Res Rev*. 2004;10(2):126-131.
11. Chu-Shore CJ, Major P, Camposano S, Muzykewicz D, Thiele EA. The natural history of epilepsy in tuberous sclerosis complex. *Epilepsia*. 2010;51(7):1236-1241.
12. Jansen FE, Vincken KL, Algra A, et al. Cognitive impairment in tuberous sclerosis complex is a multifactorial condition. *Neurology*. 2008;70(12):916-923.
13. de Vries PJ, Belousova E, Benedik MP, et al. TSC-associated neuropsychiatric disorders (TAND): findings from the TOSCA natural history study. *Orphanet J Rare Dis*. 2018;13(1):157.
14. Boer K, Crino PB, Gorter JA, et al. Gene expression analysis of tuberous sclerosis complex cortical tubers reveals increased expression of adhesion and inflammatory factors. *Brain Pathol*. 2010;20(4):704-719.
15. Mills JD, Iyer AM, van Scheppingen J, et al. Coding and small noncoding transcriptional landscape of tuberous sclerosis complex

cortical tubers: implications for pathophysiology and treatment. *Sci Rep*. 2017;7(1):8089.
16. Bartel DP. Metazoan microRNAs. *Cell*. 2018;173(1):20-51.
17. Rajman M, Schratt G. MicroRNAs in neural development: from master regulators to fine-tuners. *Development*. 2017;144(13):2310-2322.
18. Follert P, Cremer H, Beclin C. MicroRNAs in brain development and function: a matter of flexibility and stability. *Front Mol Neurosci*. 2014;7:5.
19. Mehler MF, Mattick JS. Noncoding RNAs and RNA editing in brain development, functional diversification, and neurological disease. *Physiol Rev*. 2007;87(3):799-823.
20. Agostini M, Tucci P, Killick R, et al. Neuronal differentiation by TAp73 is mediated by microRNA-34a regulation of synaptic protein targets. *Proc Natl Acad Sci USA*. 2011;108(52):21093-21098.
21. Aranha MM, Santos DM, Sola S, Steer CJ, Rodrigues CM. miR-34a regulates mouse neural stem cell differentiation. *PLoS One*. 2011;6(8):e21396.
22. Prabowo AS, Anink JJ, Lammens M, et al. Fetal brain lesions in tuberous sclerosis complex: TORC1 activation and inflammation. *Brain Pathol*. 2013;23(1):45-59.
23. Bordarier C, Lellouch-Tubiana A, Robain O. Cardiac rhabdomyoma and tuberous sclerosis in three fetuses: a neuropathological study. *Brain Dev*. 1994;16(6):467-471.
24. Park S-H, Pepkowitz SH, Kerfoot C, et al. Tuberous sclerosis in a 20-week gestation fetus: immunohistochemical study. *Acta Neuropathol*. 1997;94(2):180-186.
25. Northrup H, Krueger DA, International Tuberous Sclerosis Complex Consensus Group. Tuberous sclerosis complex diagnostic criteria update: recommendations of the 2012 International Tuberous Sclerosis Complex Consensus Conference. *Pediatr Neurol*. 2013;49(4):243-254.
26. Lim JS, Kim W-I, Kang H-C, et al. Brain somatic mutations in MTOR cause focal cortical dysplasia type II leading to intractable epilepsy. *Nat Med*. 2015;21(4):395-400.
27. Koh HY, Kim SH, Jang J, et al. BRAF somatic mutation contributes to intrinsic epileptogenicity in pediatric brain tumors. *Nat Med*. 2018;24(11):1662-1668.
28. Korotkov A, Puhakka N, Gupta SD, et al. Increased expression of miR142 and miR155 in glial and immune cells after traumatic brain injury may contribute to neuroinflammation via astrocyte activation. *Brain Pathol*. 2020;30(5):897–912.
29. Ruijter JM, Ramakers C, Hoogaars WMH, et al. Amplification efficiency: linking baseline and bias in the analysis of quantitative PCR data. *Nucleic Acids Res*. 2009;37(6):e45.
30. Korotkov A, Broekaart DWM, Van Scheppingen J, et al. Increased expression of matrix metalloproteinase 3 can be attenuated by inhibition of microRNA-155 in cultured human astrocytes. *J Neuroinflammation*. 2018;15(1):211.
31. Schneider CA, Rasband WS, Eliceiri KW. NIH Image to ImageJ: 25 years of image analysis. *Nat Methods*. 2012;9(7):671-675.
32. Agarwal V, Bell GW, Nam JW, Bartel DP. Predicting effective microRNA target sites in mammalian mRNAs. *eLife*. 2015;4:e05005.
33. Szklarczyk D, Gable AL, Lyon D, et al. STRING v11: protein-protein association networks with increased coverage, supporting functional discovery in genome-wide experimental datasets. *Nucleic Acids Res*. 2019;47(D1):D607-D613.
34. Bongaarts A, van Scheppingen J, Korotkov A, et al. The coding and non-coding transcriptional landscape of subependymal giant cell astrocytomas. *Brain*. 2020;143(1):131-149.
35. Rokavec M, Li H, Jiang L, Hermeking H. The p53/miR-34 axis in development and disease. *J Mol Cell Biol*. 2014;6(3):214-230.
36. Somel M, Guo S, Fu N, et al. MicroRNA, mRNA, and protein expression link development and aging in human and macaque brain. *Genome Res*. 2010;20(9):1207-1218.
37. Dombkowski AA, Batista CE, Cukovic D, et al. Cortical tubers: windows into dysregulation of epilepsy risk and synaptic signaling genes by microRNAs. *Cereb Cortex*. 2016;26(3):1059-1071.
38. Aranha MM, Santos DM, Xavier JM, et al. Apoptosis-associated microRNAs are modulated in mouse, rat and human neural differentiation. *BMC Genom*. 2010;11:514.
39. Mollinari C, Racaniello M, Berry A, et al. miR-34a regulates cell proliferation, morphology and function of newborn neurons resulting in improved behavioural outcomes. *Cell Death Dis*. 2015;6:e1622.
40. Fineberg SK, Datta P, Stein CS, Davidson BL. MiR-34a represses Numbl in murine neural progenitor cells and antagonizes neuronal differentiation. *PLoS One*. 2012;7(6):e38562.
41. Morgado AL, Xavier JM, Dionísio PA, et al. MicroRNA-34a modulates neural stem cell differentiation by regulating expression of synaptic and autophagic proteins. *Mol Neurobiol*. 2015;51(3):1168-1183.
42. Orlova KA, Crino PB. The tuberous sclerosis complex. *Ann N Y Acad Sci*. 2010;1184:87-105.
43. Chang TC, Wentzel EA, Kent OA, et al. Transactivation of miR-34a by p53 broadly influences gene expression and promotes apoptosis. *Mol Cell*. 2007;26(5):745-752.
44. Tazawa H, Tsuchiya N, Izumiya M, Nakagama H. Tumor-suppressive miR-34a induces senescence-like growth arrest through modulation of the E2F pathway in human colon cancer cells. *Proc Natl Acad Sci USA*. 2007;104(39):15472-15477.
45. He L, He X, Lim LP, et al. A microRNA component of the p53 tumour suppressor network. *Nature*. 2007;447(7148):1130-1134.
46. Tarasov V, Jung P, Verdoodt B, et al. Differential regulation of microRNAs by p53 revealed by massively parallel sequencing: miR-34a is a p53 target that induces apoptosis and G1-arrest. *Cell Cycle*. 2007;6(13):1586-1593.
47. Raver-Shapira N, Marciano E, Meiri E, et al. Transcriptional activation of miR-34a contributes to p53-mediated apoptosis. *Mol Cell*. 2007;26(5):731-743.
48. Lee C-H, Inoki K, Karbowniczek M, et al. Constitutive mTOR activation in TSC mutants sensitizes cells to energy starvation and genomic damage via p53. *EMBO J*. 2007;26(23):4812-4823.
49. Budanov AV, Karin M. p53 target genes sestrin1 and sestrin2 connect genotoxic stress and mTOR signaling. *Cell*. 2008;134(3):451-460.
50. Feng Z, Zhang H, Levine AJ, Jin S. The coordinate regulation of the p53 and mTOR pathways in cells. *Proc Natl Acad Sci USA*. 2005;102(23):8204-8209.
51. Armstrong LC, Westlake G, Snow JP, et al. Heterozygous loss of TSC2 alters p53 signaling and human stem cell reprogramming. *Hum Mol Genet*. 2017;26(23):4629-4641.
52. Slabakova E, Culig Z, Remsik J, Soucek K. Alternative mechanisms of miR-34a regulation in cancer. *Cell Death Dis*. 2017;8(10):e3100.
53. Maldonado M, Baybis M, Newman D, et al. Expression of ICAM-1, TNF-alpha, NF kappa B, and MAP kinase in tubers of the tuberous sclerosis complex. *Neurobiol Dis*. 2003;14(2):279-290.
54. Martin KR, Zhou W, Bowman MJ, et al. The genomic landscape of tuberous sclerosis complex. *Nat Commun*. 2017;8:15816.
55. Glenn OA, Barkovich AJ. Magnetic resonance imaging of the fetal brain and spine: an increasingly important tool in prenatal diagnosis, part 1. *AJNR Am J Neuroradiol*. 2006;27(8):1604-1611.
56. Chen CP, Su YN, Hung CC, Shih JC, Wang W. Novel mutation in the TSC2 gene associated with prenatally diagnosed cardiac rhabdomyomas and cerebral tuberous sclerosis. *J Formos Med Assoc*. 2006;105(7):599-603.
57. Saada J, Hadj Rabia S, Fermont L, et al. Prenatal diagnosis of cardiac rhabdomyomas: incidence of associated cerebral lesions of tuberous sclerosis complex. *Ultrasound Obstet Gynecol*. 2009;34(2):155-159.
58. Wortmann SB, Reimer A, Creemers JW, Mullaart RA. Prenatal diagnosis of cerebral lesions in Tuberous sclerosis complex (TSC).

Case report and review of the literature. *Eur J Paediatr Neurol*. 2008;12(2):123-126.
59. Mizuguchi M, Takashima S. Neuropathology of tuberous sclerosis. *Brain Dev*. 2001;23(7):508-515.
60. Keely PJ, Rusyn EV, Cox AD, Parise LV. R-Ras signals through specific integrin alpha cytoplasmic domains to promote migration and invasion of breast epithelial cells. *J Cell Biol*. 1999;145(5):1077-1088.
61. Wozniak MA, Kwong L, Chodniewicz D, Klemke RL, Keely PJ. R-Ras controls membrane protrusion and cell migration through the spatial regulation of Rac and Rho. *Mol Biol Cell*. 2005;16(1):84-96.
62. Pang RTK, Leung CON, Ye T-M, et al. MicroRNA-34a suppresses invasion through downregulation of Notch1 and Jagged1 in cervical carcinoma and choriocarcinoma cells. *Carcinogenesis*. 2010;31:1037-1044.
63. Ables JL, Breunig JJ, Eisch AJ, Rakic P. Not(ch) just development: notch signalling in the adult brain. *Nat Rev Neurosci*. 2011;12(5):269-283.
64. Yoon K, Gaiano N. Notch signaling in the mammalian central nervous system: insights from mouse mutants. *Nat Neurosci*. 2005;8(6):709-715.
65. Chang SJ, Weng SL, Hsieh JY, Wang TY, Chang MD, Wang HW. MicroRNA-34a modulates genes involved in cellular motility and oxidative phosphorylation in neural precursors derived from human umbilical cord mesenchymal stem cells. *BMC Med Genomics*. 2011;4:65.
66. Soni K, Gupta S, Gokhale SS, et al. Detection and knockdown of microRNA-34a using thioacetamido nucleic acid. *Nucleic Acid Ther*. 2013;23(3):195-202.
67. Wu J, Bao J, Kim M, et al. Two miRNA clusters, miR-34b/c and miR-449, are essential for normal brain development, motile ciliogenesis, and spermatogenesis. *Proc Natl Acad Sci USA*. 2014;111(28):E2851-E2857.
68. Bernardo BC, Gao X-M, Winbanks CE, et al. Therapeutic inhibition of the miR-34 family attenuates pathological cardiac remodeling and improves heart function. *Proc Natl Acad Sci USA*. 2012;109(43):17615-17620.
69. Bernardo BC, Gregorevic P, Ritchie RH, McMullen JR. Generation of microRNA-34 sponges and tough decoys for the heart: developments and challenges. *Front Pharmacol*. 2018;9:1090.
70. Meng L, Liu C, Lü J, et al. Small RNA zippers lock miRNA molecules and block miRNA function in mammalian cells. *Nat Commun*. 2017;8:13964.
71. Rupaimoole R, Slack FJ. MicroRNA therapeutics: towards a new era for the management of cancer and other diseases. *Nat Rev Drug Discov*. 2017;16(3):203-222.
72. Kumar B, Yadav A, Lang J, Teknos TN, Kumar P. Dysregulation of microRNA-34a expression in head and neck squamous cell carcinoma promotes tumor growth and tumor angiogenesis. *PLoS One*. 2012;7(5):e37601.
73. French JA, Lawson JA, Yapici Z, et al. Adjunctive everolimus therapy for treatment-resistant focal-onset seizures associated with tuberous sclerosis (EXIST-3): a phase 3, randomised, double-blind, placebo-controlled study. *Lancet*. 2016;388(10056):2153-2163.
74. Feliciano DM. The neurodevelopmental pathogenesis of Tuberous Sclerosis Complex (TSC). *Front Neuroanat*. 2020;14:39.

SUPPORTING INFORMATION

Additional supporting information may be found online in the Supporting Information section.

How to cite this article: Korotkov A, Sim NS, Luinenburg MJ, et al. MicroRNA-34a activation in tuberous sclerosis complex during early brain development may lead to impaired corticogenesis. *Neuropathol Appl Neurobiol*. 2021;47:796–811. https://doi.org/10.1111/nan.12717